Int j simul model 16 (2017) 2, 229-240
ISSN 1726-4529 Original scientific paper

FINITE ELEMENT ANALYSIS FOR RUTTING PREDICTION OF ASPHALT CONCRETE PAVEMENT UNDER MOVING WHEEL LOAD

Wang, Y.[*,#]; Lu, Y. J.[*]; Si, C. D.[*] & Sun, T. C.[**]
[*] Key Laboratory of Traffic Safety and Control in Hebei, Shijiazhuang Tiedao University, 17 Northeast, Second Inner Ring, Shijiazhuang, P. R. China
[**] College of Engineering, University of Alaska Anchorage, Anchorage, AK 99508, United States
E-Mail: jtxwy@163.com ([#] Corresponding author)

Abstract
In order to improve the accuracy of the finite element rutting prediction model and evaluate the influences of truck parameters (wheel set, axle set, vehicle travel speed, and tire pressure) on rutting, a modified 3D pavement model was built in this study. The new model adopted a moving wheel load to perform repeated loading on the pavement, and the strain-hardening formulation was used as the creep law of the asphalt mixture. Results indicate that the front axle of single-rear-axle truck is as important as the rear axle to pavement rutting. The dual-axle truck can more easily cause pavement rutting than the single-axle truck, and the dual-axle wheel load increases rutting by 33 %. Moreover, the vehicle running at a slow speed can increase pavement rutting by a large margin. When the movement speed of wheel load decreases from 80 km/h to 60 km/h, the rutting is increased by 60 %. The high tire pressure generates considerable depression. When the tire pressure increases from 0.70 MPa to 0.90 MPa, the maximum depression on pavement increases by 7 %. The conclusions provide a reference for the pavement design and shear resistance design of asphalt mixture.
(Received in August 2016, accepted in January 2017. This paper was with the authors 2 months for 2 revisions.)

Key Words: Rutting, Moving Wheel Load, Finite Element, Strain Hardening Formulation

1. INTRODUCTION

As one of the main modern modes of transportation, road transportation exhibits prominent advantages of manoeuvrability, flexibility, and adaptability to traffic volume. Hence, road infrastructures have been a main emphasis when constructing traffic facilities. In modern high-grade road construction, the asphalt concrete pavement has been favoured by various countries worldwide and extensively applied due to its favourable mechanical property, flat and wearable surface, comfortable travelling performance, and good construction workability. Most expressways in China have used asphalt concrete or modified asphalt concrete as pavement materials.

With increasing traffic volume, overload vehicle, and canalized traffic, asphalt pavement failure is increasingly serious, which; such failure is common in asphalt pavements in various countries worldwide [1]. Rutting, a longitudinal groove along the road, is one of the main failures to asphalt pavement to date [2]. Among numerous pavement failures, rutting presents more serious hazards in particular. From the viewpoint of road users, first, under lane change or overtaking circumstances, rutting directly decreases the lateral stability and manoeuvrability of vehicles; second, rutting easily accumulates water in rainy days, and the water-accumulated rutting will easily generate hydroplaning of vehicles. From the angle of pavement structure, rutting occurs on the top pavement layer and often endangers the intermediate, lower, and basement pavement layers. Serious rutting will also result in structural failure of asphalt pavement.

Rutting is not a new pavement failure. However, under existing road transportation conditions, the speed and magnitude of rutting considerably exceed common expectations,

and rutting becomes a main problem in road engineering field. Studies on structural behaviours of pavements have gradually increased in recent years. Researchers have begun to recognize that rutting can be prevented and controlled, but only when rutting performance index and design method are systematically improved. Thus, developing a reasonable model to predict rutting of asphalt concrete pavement forms the groundwork for future relevant research.

2. STATE OF THE ART

To date, the main rutting prediction models are analytical methods based on layered theory; according to different assumptions about mechanical behaviours of asphalt mixture, these models can be classified into layer strain methodology [3] or viscoelastic theory [4]. Prediction using nonlinear viscoelastic theory based on the generalized Maxwell viscoelastic model is the most accurate. Nevertheless, the generalized Maxwell viscoelastic model cannot yet describe the mechanical behaviours of asphalt concrete materials well. Furthermore, the plastic elements of this model still need further improvement.

The main cause of pavement rutting lies in the nonlinear mechanical properties of paving materials. The finite element method can overcome defects of the layered theory and simulate mechanical behaviours of nonlinear materials accurately. From the perspective of computational method, finite element analysis is a new development orientation for rutting prediction [5].

The longitudinal dimension of a pavement is remarkably higher than its horizontal and vertical measurements. The 2D finite element model can significantly improve the computing efficiency, thereby its current usage. In their rutting experiment where asphalt mixture specimen was used as prototype, Arabani et al. [6] established a prediction model to evaluate the antirutting performance of glass asphalt concrete. The creep behaviour of the asphalt mixture was described by the time-hardening formulation. To further improve computing efficiency, they transformed the dynamic wheel load into a static-accumulated load. For the transverse section of pavement, the actual wheel load used is pulse load, and the static-accumulated load could not accurately reflect this feature of the wheel load [7].

Under the effect of wheel load, pavement should be under complicated spatial stress state. The 2D finite element model simplifies the practical problem into a plane strain problem, and its prediction effect will certainly be influenced. Compared with 2D model, 3D model can more accurately simulate the mechanical behaviours of pavement. With the continuously improved computing efficiency of computer, many scholars have used 3D finite element model to predict pavement rutting.

Pérez et al. [8] used nonlinear elastic-plastic asphalt concrete model to predict permanent deformation of pavement and analyse the antirutting and antifatigue performances of base materials. In their model, the wheel load was still processed as a static force. Some scholars have modified the application mode of wheel load and repeatedly applied pulse load at fixed position of pavement model to simulate the instantaneous effect of wheel load on pavement. On the basis of the constitutive relation of elastic-plastic material, Allou et al. [9] used finite element method to predict the rutting of a low traffic pavement. Leonardi [10, 11] predicted the influence of aircraft landing process on rutting on an airport pavement, and Imaninasab et al. [12, 13] evaluated the antirutting performance of asphalt concrete pavement. Pulse load belongs to nonconstant load, so it was worthy of discussion that Leonardi and Imaninasab et al. selected time hardening formulation as the creep law of asphalt mixture when they applied pulse load to pavement.

In spatial 3D, an actual wheel load is a moving load, and none of the above models have used this load mode. In mechanical response research of pavement structure, moving wheel

load is applied on pavement [14-16]; on this basis, some scholars have explored rutting prediction by using moving load. Zhu and Sun [17] proposed a rutting prediction method of asphalt pavement based on two-stage constitutive model of viscoelastic-viscoplastic damage, and they used moving wheel load for loading. Their model only conducts the rutting prediction of asphalt mixture specimen in rutting experiment but not the modelling or simulation of actual pavement model. Zopf et al. [18] used one Maxwell element and two fractional Maxwell elements to describe the viscoelastic behaviours of asphalt mixture; they also established a pavement model under moving load and predicted rutting. Their research proposed the modelling method but presented no discussion about the influence of vehicle parameters on rutting.

The wheel load mode on finite element model for rutting prediction can be continuously improved by using actual wheel load as the reference. This study uses ABAQUS software to establish a 3D pavement model so as to realize the reciprocal application of wheel load on the pavement and evaluate influences of truck parameters (wheel set, axle set, vehicle travel speed, and tire pressure) on rutting. This study is further organized as follows. Section 3 introduces the simulation model for pavement rutting and highlights the application of a moving wheel load. Section 4 provides the prediction of pavement rutting under the effect of a moving wheel load and the effects of relevant parameters. Conclusions are drawn in Section 5.

3. METHODOLOGY

3.1 Computational domain and domain discretion

The main structural layers of expressway include pavement layer, base layer, subbase, and subgrade, where pavement layer is directly affected by vehicle load. Most rutting is formed through depression and lateral displacement generated by pavement layer materials under the effect of wheel load. Given the significant lateral creep displacement on pavement materials, upheaval occurs on two rutting sides, and a typical cross section of pavement suffering from rutting damage is shown in Fig. 1 [19].

Figure 1: Typical cross section of pavements damaged by rutting.

A pavement structure from a segment of China's G45 highway was used as prototype in the establishment of pavement model using the ABAQUS software. In consideration that pavement layer was paved in three layers, and compositions of asphalt mixtures at different layers were different, the pavement layer in the model was divided into three structural layers, namely, top pavement layer, intermediate pavement layer, and bottom-surface layer. The pavement model structure is shown in Fig. 2, and the division of computational meshes is shown in Fig. 3. The direction of the *X*-axis of the model is the driving direction, the direction

of *Y*-axis is the transverse direction of pavement, and the negative direction of *Z*-axis is the depth direction. Lengths of *Y*- and *Z*-directions in the model were 1.4 and 2.0 m, respectively. The length of *X*-direction, marked as *L*, was determined through a trial calculation. The displacements of two longitudinal sides in *X*-direction, two transverse sides in *Y*-direction, and the base in *Z*-direction were all zero.

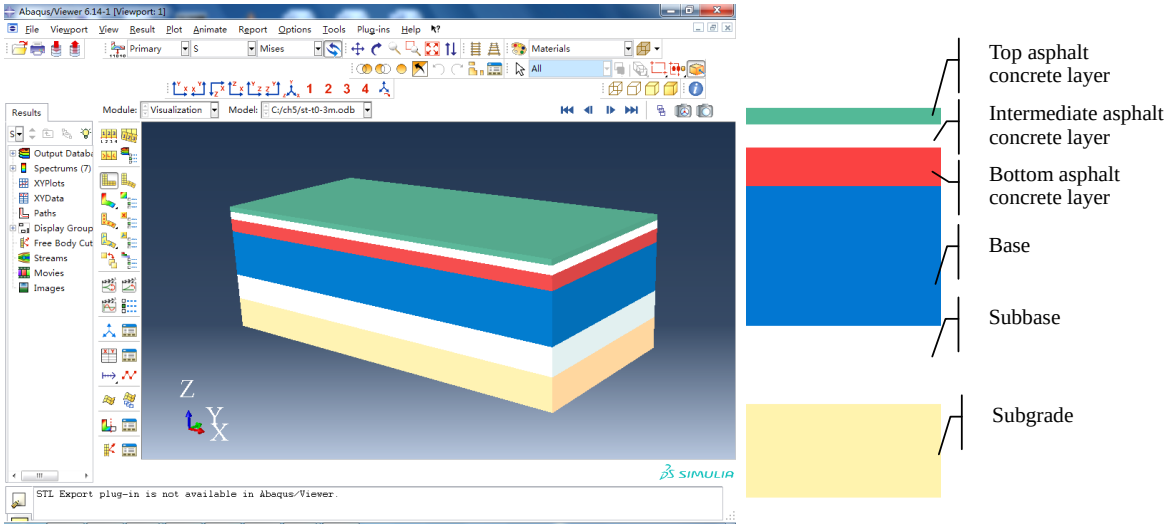

a) Pavement model b) Pavement structural layers

Figure 2: Pavement modelled using the ABAQUS software.

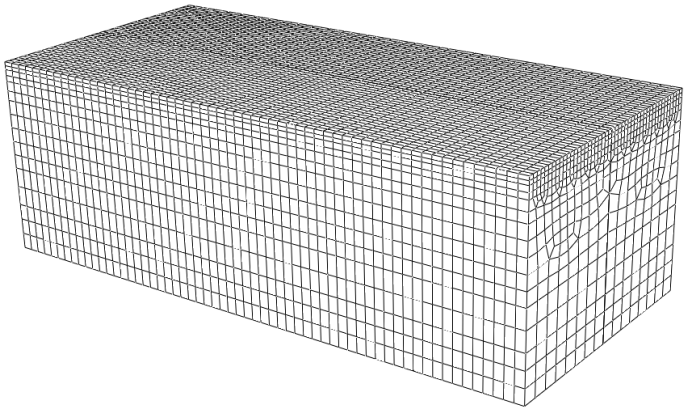

Figure 3: Computational mesh for the pavement model.

3.2 Material model and parameters

The gradual enlargement of material deformation with time under certain temperature and small stress is called creep deformation. Asphalt mixture is a typical viscous-elastic material that can exert significant creep effect under normal temperature. To describe the creep behaviour of the material, its total strain $\varepsilon(t)$ is decomposed into elastic strain ε_e and non-elastic strain ε_{in} [20], that is,

$$\varepsilon(t) = \varepsilon_e + \varepsilon_{in} \tag{1}$$

where ε_{in} includes plastic strain ε_p and creep strain ε_c, such that,

$$\varepsilon_{in} = \varepsilon_p + \varepsilon_c \tag{2}$$

Assuming that the pavement has not entered its yield phase under the wheel load effect, then $\varepsilon_p = 0$ and $\varepsilon(t)$ can be expressed as follows:

$$\varepsilon(t) = \varepsilon_e + \varepsilon_c \tag{3}$$

where ε_e is unrelated to time. The relation between ε_e and strain σ and between ε_e and elastic modulus E can be expressed as follows:

$$\varepsilon_e = \frac{\sigma}{E} \tag{4}$$

ε_c is a function of time t, temperature T, and σ, that is,

$$\varepsilon_c = f(t,\ T,\ \sigma) = f_1(t)\, f_2(T)\, f_3(\sigma) \tag{5}$$

Furthermore, assuming that asphalt mixture is undergoing primary creep under wheel load effect, ε_c under fixed temperature can be expressed as follows:

$$\varepsilon_c = f(t,\ \sigma) = \frac{A}{m+1}\sigma^n t^{m+1} \tag{6}$$

where A, m, and n are the creep parameters of the material.

Creep strain rate can be obtained by computing the time differential in Eq. (6):

$$\frac{d\varepsilon_c}{dt} = A\sigma^n t^m \tag{7}$$

Eq. (7) refers to the time-hardening formula of the creep model, and it is commonly used for creep analysis under constant load. For creep analysis under nonconstant load, the strain-hardening formula of the creep model is usually used:

$$\frac{d\varepsilon_c}{dt} = \left\{ A\sigma^n \left[(m+1)\varepsilon_c \right]^m \right\}^{\frac{1}{m+1}} \tag{8}$$

Thus, the creep strain rate in Eq. (8) is related with the cumulant values of creep strain but unrelated with time. For pavement rutting prediction under moving load, Eq. (8) should be selected for the creep law of the asphalt mixture. In this study, the other pavement materials of the established model were assumed isotropic and linear elastic. The pavement structural and material parameters are shown in Tables I and II, respectively.

Table I: Structural and material parameters of the pavement layers.

Pavement layer	**Thickness** (cm)	***A***	***m***	***n***	**Modulus** (Pa)	**Poisson ratio**
Top	4	1.464 e-5	0.336	-0.502	5.26 e8	0.45
Intermediate	6	4.802 e-6	0.595	-0.532	4.4 e8	0.40
Bottom	10	1.956 e-8	0.830	-0.562	7.1 e8	0.35

Table II: Structural and material parameters of the base, subbase, and subgrade layers.

Pavement layer	**Thickness** (cm)	**Modulus** (Pa)	**Poisson ratio**
Base	36	1.6 e9	0.35
Subbase	20	8 e8	0.20
Subgrade	—	3 e7	0.40

3.3 Application of wheel load

A single tire of heavy truck bore 25 kN load, the contact zone between tire and pavement was a circle with diameter of 21.30 cm, the contact stress was uniformly distributed vertical stress, and the contact stress was 0.70 MPa according to the tire load and the area of contact zone. The actual form of wheel set of a rear axle of heavy truck was dual-wheel, and the distance of circular centres of two tire-pavement contact zones was 34.60 cm. In the absence of significant discussion, the wheel load in this study is single-axle dual-wheel.

The wheel load was positioned symmetrically with the X-axis and moved along it at each loading process, as shown in Fig. 4. The tire force moved from the left to the right side of the pavement at uniform velocity so as to complete a loading process. The time interval for the wheel load applied to reach the same position is marked as Δt, and the time needed to

complete one loading process is marked t_1. The initial time of loading at N^{th} time is $t = N\Delta t$, and the time to complete this loading is $t = N\Delta t + t_1$.

Thus, to improve simulation efficiency, the Δt and L values should be small. However, the creep strain of asphalt mixture is related with time, and Δt must be prudently selected. Similarly, considerably small L value will affect the stress state of the internal nodes of the pavement, thereby the computing error of creep strain. Reasonable Δt and L values should be determined through trial calculation so as to guarantee the accuracy of the rutting prediction result.

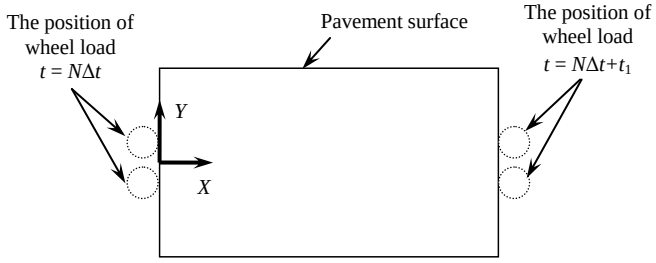

Figure 4: Plane position of the wheel load for each loading process.

3.4 Feature sections and points

Mechanical behaviours on the $x = L / 2$ section show the most approximate physical representation of the pavement, also known as the feature section. On this feature section, three feature points are defined and subsequently used to analyse the permanent deformation of the pavement. The positions of the feature section and feature points for the pavement under the dual-wheel load is shown in Fig. 5, where A is the central point in tire-pavement contact zone, B is the maximum upheaval point at the external side of tire force, and C is location on the X-axis.

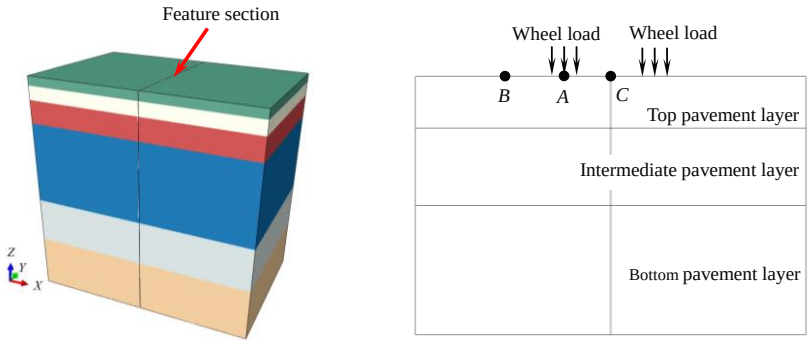

a) Position of feature section b) Position of feature points

Figure 5: Positions of the feature section and points.

3.5 Determination of Δt and L

A trial calculation for the $L = 10$ m model was performed. The wheel load was forced once on the pavement at a velocity of 80 km/h, which resulted in $t_1 = 0.47$ s. The pavement displacements in Z direction at different periods of the loading process are shown in Fig. 6.

Trial calculation results indicated that the creep process was the longest at point A, as evidenced by the time travel curves of the principal creep strains (CEPs) at this point (Fig. 7).

Furthermore, prior to 0.15 s, the wheel load was distant from point A; thus, its effect can be ignored. At 0.15-0.18 s, which was the loading phase of point A, the peak values of CEPs in all directions occurred at 0.18 s. The unloading phase of point A was after 0.18 s. Notable time differences were observed among CEPs in different directions.

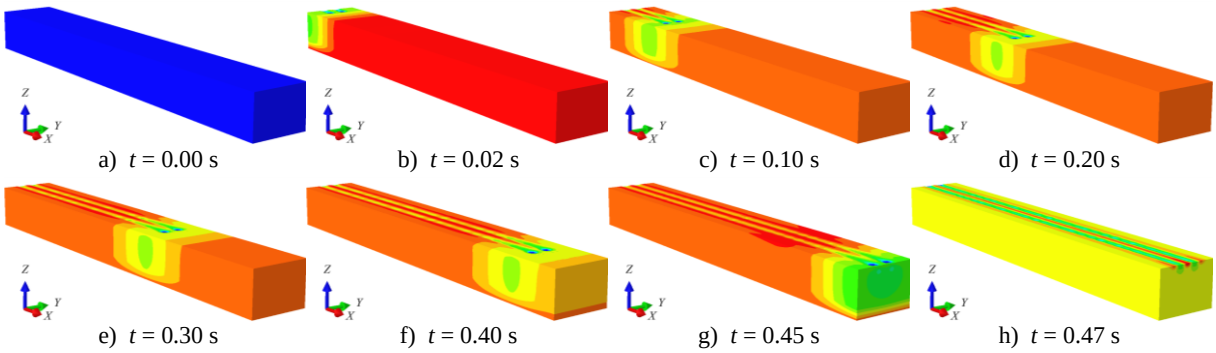

a) t = 0.00 s b) t = 0.02 s c) t = 0.10 s d) t = 0.20 s

e) t = 0.30 s f) t = 0.40 s g) t = 0.45 s h) t = 0.47 s

Figure 6: Pavement displacements in Z-direction at different periods.

After 0.18 s, CEP1 firstly reduced and then slightly increased with time. After 0.32 s, CEP1 gradually stabilized at about -140 $\mu\varepsilon$. During the initial loading phase, CEP2 was under a tension state, and it rapidly shifted to a compressive state after 0.18 s. An extreme value of compressive strain was observed at 0.24 s. After 0.32 s, CEP2 gradually stabilized at about -45 $\mu\varepsilon$. Finally, CEP3 exhibited a small lowering process after 0.18 s, increased with time, and gradually stabilized at about 180 $\mu\varepsilon$ after 0.35 s.

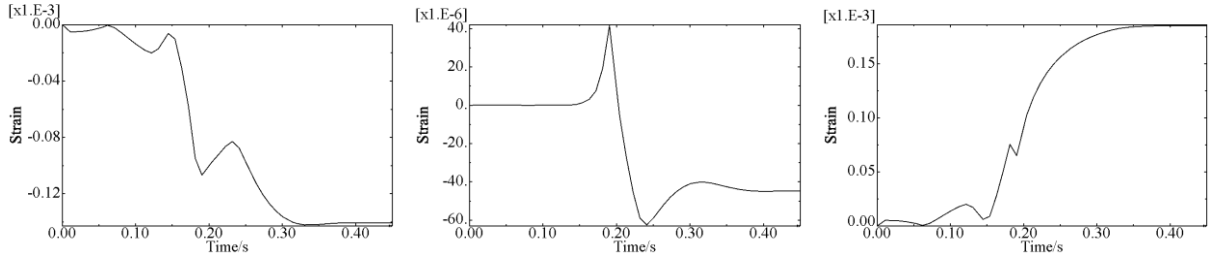

a) CEP1 b) CEP2 c) CEP3

Figure 7: Principal creep strain (CEP) time travel curves of Point *A*.

Eq. (8) indicates that creep strain rate is related with the cumulant value of the creep strain when the strain-hardening formulation is used to describe the creep behaviours of the pavement layer material. Hence, to determine Δt, its influence on the material loading-unloading process should also be considered. Trial calculations results indicated that one-time loading-unloading process of pavement layer material lasted 0.25 s. In practical road transportation conditions, excluding that for the multi-axle set, the loading time interval for the wheel load is not be lower than 0.25 s. Hence, Δt = 0.25 s.

Results further showed that L can be appropriately reduced so as to reduce the model scale. The dimensions used by Wang and Al-Qadi [14] were used as reference, which confirmed that L = 3 m.

4. RESULT ANALYSIS AND DISCUSSION

4.1 Rutting under standard working condition

Loading wheel load to the pavement at a velocity of 80 km/h for 500,000 times was used as the standard working condition. Results of the rutting simulation for the feature section are shown in Fig. 8 and Table III.

Table III: Results of rutting prediction for the feature section.

Maximum upheaval (mm)	**Maximum depression** (mm)	**Rutting** (mm)	**Ratio of Maximum depression to rutting** (%)
5.63	17.89	23.52	76

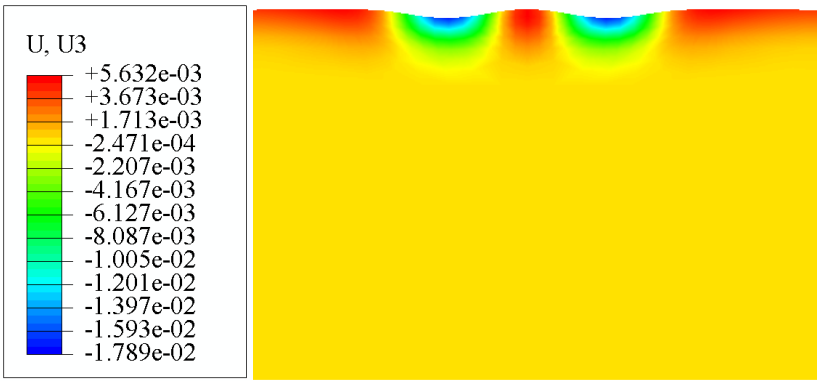

Figure 8: Results of the rutting simulation for the feature section under standard working condition.

The rutting simulation results of feature section under standard working condition (Fig. 8 and Table III) indicated the presence of the following features. The depressions appeared under the tire-pavement contact zone, and the upheavals appeared at two sides of each depression. The variation rule of pavement elevation was identical with the observed experimental result in Fig. 1. Point *A* was the maximum pavement depression point, and point *C* was the highest pavement upheaval point. Pavement upheaval also appeared at point *B*, but upheaval amplitude was smaller than that at point *C*. The maximum elevation difference between pavement depression and upheaval was recorded as rutting, and depression was the main part of rutting.

For further analysis of differences between different layers in permanent deformation, statistical data of the permanent deformations of layers at lower parts of feature points are provided in Table IV. The results showed that permanent deformation of intermediate pavement layer occupied the highest proportion in permanent pavement deformation, which was in accordance with the prediction results in [21]. Thus, improving the ability of intermediate pavement layer in resisting permanent deformation is considerably significant to reduce pavement rutting.

Table IV: Permanent pavement deformation under standard working condition.

Pavement Layer	**Lower part of point *A***		**Lower part of point *B***		**Lower part of point *C***	
	Deformation (mm)	**Proportion** (%)	**Deformation** (mm)	**Proportion** (%)	**Deformation** (mm)	**Proportion** (%)
Top	-5.71	32	1.69	31	0.64	11
Intermediate	-8.28	46	2.50	46	3.08	55
Bottom	-3.90	22	1.19	22	1.91	34

4.2 Influence of front axle of heavy truck on pavement rutting

The front axle of heavy truck is single-wheel set. Under full load condition, although the axle load is smaller than the rear axle, the operating status of each tire is not different from that of rear-axle tire. To analyse the influence of front-axle tire on rutting, a wheel load of single-wheel set was repeatedly loaded to the pavement for 500,000 times at velocity of 80 km/h. The rutting simulation result of feature section is shown in Fig. 9.

Fig. 9 indicates that under single-wheel tire force, the maximum depression of feature section was 17.38 mm, and the upheaval heights at two rutting sides were both 3.13 mm. Comparison with the simulation result in Fig. 8 showed slight difference between the two working conditions in rutting prediction result. This result sufficiently indicated that front-axle tire was as important as rear-axle tire to rutting under the same operating condition. Hence, in road transportation management, attention must be given to the axle load of front axle of the truck.

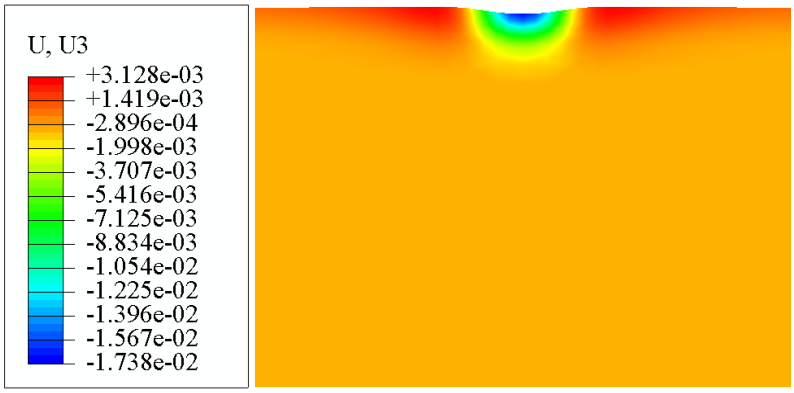

Figure 9: Rutting simulation result of feature section under wheel load of a single-wheel set.

4.3 Influence of axle set on pavement rutting

The wheel load a dual-axle model was applied to the pavement for 250,000 times at a velocity of 80 km/h. The axle distance of dual-axle model was 1.3 m. Simulation results are shown in Fig. 10.

The rutting prediction result of feature section under the dual-axle wheel load increased by 33 %. The maximum depression under this working condition reached 23.77 mm. A 5.88 mm increase was noted compared with rutting simulation under standard working condition. Pavement upheavals also increased; the upheaval was 7.44 and 6.87 mm at points *C* and *B*, respectively.

Under the effect of the dual-axle wheel load, the minimum time interval for wheel loading was less than 0.06 s. According to the analysis presented in Section 3.5, the wheel load was loaded to the pavement at such small time intervals, so that the asphalt mixture started another loading process even when the last unloading process was not totally completed. Such loading form eventually increased the chances of pavement failure. Hence, under the same tire operating conditions, the wheel load of dual-axle model can more easily cause pavement rutting than that with the single axle.

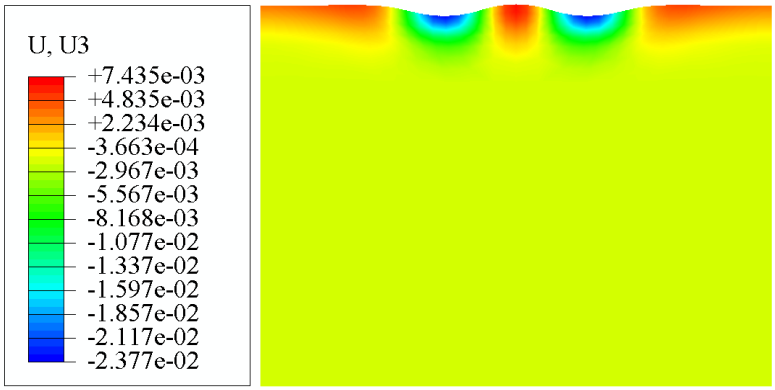

Figure 10: Results from rutting simulation (feature section) under the wheel load of a dual-axle model.

4.4 Influence of travel speed on pavement rutting

The wheel load was forced to the pavement for 500,000 times at a velocity of 60 km/h to evaluate the influence of travel speed on rutting. Rutting simulation result of the feature section is shown in Fig. 11. When the truck travelled at low speed, the time for each loading-unloading process for the pavement increased, which also increased the likelihood of permanent deformation for the asphalt concrete. Calculation results indicated that compared with standard working condition, at the velocity of 60 km/h, rutting of the feature section can

increase by 60 %. The maximum depression and maximum upheaval of the feature section were 25.69 and 11.92 mm, respectively. Thus, rutting at intersections is closely related with the long-time effect of wheel loads.

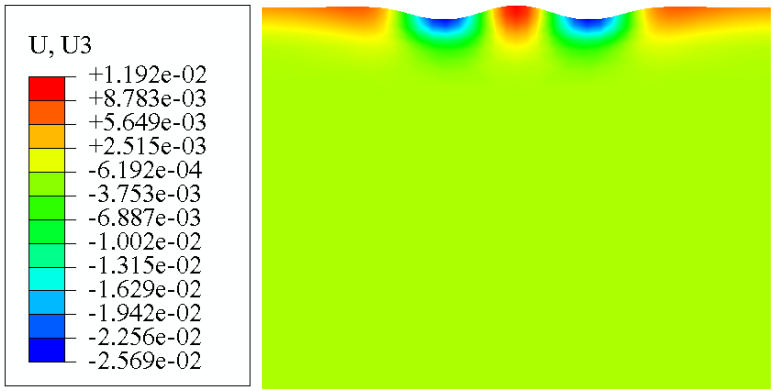

Figure 11: Results from rutting simulation (feature section) at the travel speed of 60 km/h.

4.5 Influence of tire pressure on pavement rutting

To evaluate the influence of tire pressure on rutting, a wheel load under 0.90 MPa tire pressure was selected to load on the pavement [22]. Under this working condition, each tire bore 25 kN load, the contact stress was 0.90 MPa, the tire-pavement contact zone was still circular, and its area was determined according to the tire load and contact stress. This wheel load was loaded to the pavement for 500,000 times at velocity of 80 km/h. The rutting simulation result of feature section is shown in Fig. 12.

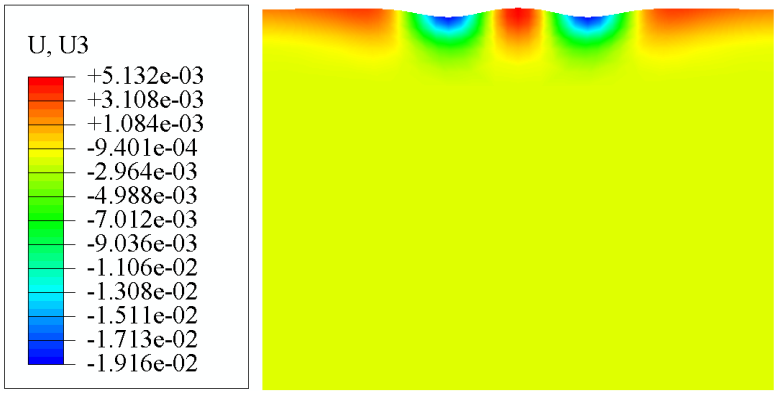

Figure 12: Results of rutting simulation (feature section) under a wheel load of 0.90 MPa tire pressure.

Simulation result indicated that under a 0.90 MPa tire pressure, the maximum depression and maximum upheaval of the feature section were 19.16 and 5.13 mm, respectively. Compared with the simulation result under standard working condition, increase in tire pressure also increased maximum depression by 7 %, whereas the upheaval amplitude slightly decreased. Despite that high tire pressure exerted no significant change on rutting, the increased depression indicated the considerable damage to the pavement. Therefore, high tire pressure can still shorten the service life of a pavement. When defining overlimit behaviours of the vehicle, the overlimit of tire pressure should be incorporated as an assessment index.

5. CONCLUSIONS

On the basis of the analysis on the creep rule of asphalt mixture, an improved rutting prediction model was established in this study using ABAQUS software. Subsequently, 3D

finite element simulation of pavement rutting under moving wheel load was conducted to evaluate the influence of vehicle parameters on pavement rutting accurately, and the main conclusions are shown as follows:

(1) Moving wheel load is a nonconstant load. The creep rule of asphalt mixture should be the strain-hardening formulation because this formulation is unrelated with time. When single-axle wheel load is running at normal speed, asphalt mixture finishes a complete loading-unloading process within a loading cycle. The time interval of wheel load application to the pavement in finite element model should be strictly controlled. On the premise that the asphalt mixture can complete the loading-unloading process, the time interval should be a small value so as to improve solving efficiency.

(2) Under standard working condition, pavement deformation presents depressions and upheavals simultaneously. Depression appears under the tire-pavement contact zone, and its maximum value is obtained at point *A*. Depression magnitude is more than three times of that of upheaval.

(3) Permanent deformations of top, intermediate, and bottom pavement layers are not uniformly distributed; the deformation of intermediate pavement layer is the main part of rutting. Controlling the permanent deformation of intermediate pavement layer should be the main principle of improving the antirutting ability of the pavement.

(4) The front axle of single-rear-axle truck exerts the same important influence as rear axle on pavement rutting, and dual-axle wheel load can more easily cause pavement rutting than single-axle wheel load. Under the same tire operating condition, no significant difference exists between rutting caused by single-wheel set and that by dual-wheel set. Double-axle wheel load increases rutting by 33 %.

(5) Vehicle traveling at low velocity can increase pavement rutting by a large margin. The antirutting performance of the pavement should be improved, especially for the road with vehicles travelling at low velocity. High tire pressure generates high maximum depression. When the overlimit behaviour of the vehicle is defined, the overlimit of tire pressure should be incorporated as an assessment index.

In this study, the established model is more approximate to practical situation than the original model. Research conclusions can provide reference for the pavement structure design and the shear resistance design of asphalt mixture. In the established model, the selected wheel load was circularly uniformly distributed vertical stress without consideration of horizontal contact stress or non-uniformity of contact stress distribution inside the tire-pavement contact zone. Future research should apply three-directional complicated contact stress on the pavement and conduct rutting prediction for other working conditions, such as acceleration, deceleration, and serious overloading.

ACKNOWLEDGEMENTS

This study was supported by the National Natural Science Foundation of China (Grant Nos. 11302138, 11472180, and 11572207).

REFERENCES

[1] Yang, S.; Chen, L.; Li, S. (2015). *Dynamics of Vehicle-Road Coupled System*, Springer-Verlag, Berlin

[2] Abed, A. H.; Al-Azzawi, A. A. (2012). Evaluation of rutting depth in flexible pavements by using finite element analysis and local empirical model, *American Journal of Engineering and Applied Sciences*, Vol. 5, No. 2, 163-169, doi:10.3844/ajeassp.2012.163.169

[3] Barksdale, R. D. (1972). Laboratory evaluation of rutting in base course materials, *Proceedings of the Third International Conference on the Structural Design of Asphalt Pavements*, 161-174

[4] Sousa, J. B.; Weissman, S. L. (1994). Modeling permanent deformation of asphalt-aggregate mixes, *Journal of the Association of Asphalt Paving Technologist*, Vol. 63, 224-257
[5] Peng, M. J.; Xu, Z. H. (2004). Methods of rutting prediction in asphalt pavements, *Journal of Tongji University (Natural Science)*, Vol. 32, No. 11, 1457-1460
[6] Arabani, M.; Jamshidi, R.; Sadeghnejad, M. (2014). Using of 2D finite element modeling to predict the glasphalt mixture rutting behavior, *Construction and Building Materials*, Vol. 68, 183-191, doi:10.1016/j.conbuildmat.2014.06.057
[7] Wang, Y.; Lu, Y. J.; Si, C. D. & Sung, P. (2016). Tire-pavement coupling dynamic simulation under tire high-speed-rolling condition, *International Journal of Simulation Modelling*, Vol. 15, No. 2, 236-248, doi:10.2507/IJSIMM15(2)4.332
[8] Pérez, I.; Medina, L.; del Val, M. A. (2016). Nonlinear elasto-plastic performance prediction of materials stabilized with bitumen emulsion in rural road pavements, *Advances in Engineering Software*, Vol. 91, 69-79, doi:10.1016/j.advengsoft.2015.10.009
[9] Allou, F.; Petit, C.; Chazallon, C.; Hornych, P. (2010). Shakedown approaches to rut depth prediction in low-volume roads, *Journal of Engineering Mechanics*, Vol. 136, No. 11, 1422-1434, doi:10.1061/(ASCE)EM.1943-7889.0000165
[10] Leonardi, G. (2015). Finite element analysis for airfield asphalt pavements rutting prediction, *Bulletin of the Polish Academy of Sciences – Technical Sciences*, Vol. 63, No. 2, 397-403, doi:10.1515/bpasts-2015-0045
[11] Leonardi, G. (2014). Finite element analysis of airfield flexible pavement, *Archives of Civil Engineering*, Vol. 60, No. 3, 323-334, doi:10.2478/ace-2014-0022
[12] Imaninasab, R.; Bakhshi, B. (2015). Rutting analysis of modified asphalt concrete pavements, *Proceedings of the Institution of Civil Engineers – Construction Materials*, Ahead of Print, 1-12, doi:10.1680/coma.15.00015
[13] Imaninasab, R.; Bakhshi, B.; Shirini, B. (2016). Rutting performance of rubberized porous asphalt using Finite Element Method (FEM), *Construction and Building Materials*, Vol. 106, 382-391, doi:10.1016/j.conbuildmat.2015.12.134
[14] Wang, H.; Al-Qadi, I. L. (2013). Importance of nonlinear anisotropic modeling of granular base for predicting maximum viscoelastic pavement responses under moving vehicular loading, *Journal of Engineering Mechanics*, Vol. 139, No. 1, 29-38, doi:10.1061/(ASCE)EM.1943-7889.0000465
[15] Breakah, T. M.; Williams, R. C. (2015). Stochastic finite element analysis of moisture damage in hot mix asphalt, *Materials and Structures*, Vol. 48, No. 1, 93-106, doi:10.1617/s11527-013-0170-x
[16] Wollny, I.; Behnke, R.; Villaret, K.; Kaliske, M. (2016). Numerical modelling of tyre-pavement interaction phenomena: coupled structural investigations, *Road Materials and Pavement Design*, Vol. 17, No. 3, 563-578, doi:10.1080/14680629.2015.1094399
[17] Zhu, H.; Sun, L. (2013). Mechanistic rutting prediction using a two-stage viscoelastic-viscoplastic damage constitutive model of asphalt mixtures, *Journal of Engineering Mechanics*, Vol. 139, No. 11, 1577-1591, doi:10.1061/(ASCE)EM.1943-7889.0000598
[18] Zopf, C.; Garcia, M. A.; Kaliske, M. (2015). A continuum mechanical approach to model asphalt, *International Journal of Pavement Engineering*, Vol. 16, No. 2, 105-124, doi:10.1080/10298436.2014.927065
[19] Rushing, J. F.; Darabi, M. K.; Rahmani, E.; Little, D. N. (2017). Comparing rutting of airfield pavements to simulations using pavement analysis using nonlinear damage approach (PANDA), *International Journal of Pavement Engineering*, Vol. 18, No. 2, 138-159, doi:10.1080/10298436.2015.1039007
[20] Perl, M.; Uzan, J.; Sides, A. (1983). Visco-elasto-plastic constitutive law for a bituminous mixture under repeated loading, *Transportation Research Record*, Vol. 911, 20-27
[21] Hu, X. D.; Zhong, S.; Walubita, L. F. (2015). Three-dimensional modelling of multilayered asphalt concrete pavement structures: strain responses and permanent deformation, *Road Materials and Pavement Design*, Vol. 16, No. 3, 727-740, doi:10.1080/14680629.2015.1028968
[22] Wang, Y.; Sun, T.; Lu, Y.; Si, C. (2016). Prediction for tire-pavement contact stress under steady-state conditions based on 3D finite element method, *Journal of Engineering Science and Technology Review*, Vol. 9, No. 4, 17- 25